Infrared Spectroscopic and Density Functional Theory Studies on the CO Dissociation by Scandium and Yttrium Dimers

Ling Jiang and Qiang Xu*

National Institute of Advanced Industrial Science and Technology, Ikeda, Osaka 563-8577, Japan and Graduate School of Science and Technology, Kobe University, Nada Ku, Kobe, Hyogo 657-8501, Japan

Received: January 14, 2006; In Final Form: March 2, 2006

Reactions of laser-ablated scandium and yttrium atoms with dilute carbon monoxide molecules in solid argon have been investigated using matrix-isolation infrared spectroscopy. On the basis of the results of the isotopic substitution, the change of laser power and CO concentration and the comparison with density functional theory (DFT) calculations, the absorption at 1193.4 cm^{-1} is assigned to the C−O stretching vibration of the $Sc_2[\eta^2(\mu_2\text{-C,O})]$ molecule, which has a single bridging CO that is tilted to the side. This CO-activated molecule undergoes ultraviolet−visible photoinduced rearrangement to the CO-dissociated molecule, $c\text{-}Sc_2(\mu\text{-C})(\mu\text{-O})$. The cyclic $c\text{-}Sc_2(\mu\text{-C})(\mu\text{-O})$ molecule has a bridging carbon on one side of the Sc_2 unit and a bridging oxygen on the other. The analogous $Y_2[\eta^2(\mu_2\text{-C,O})]$ molecule has not been observed, but the CO-dissociated $c\text{-}Y_2(\mu\text{-C})(\mu\text{O})$ molecule has been observed in the Y + CO experiments. DFT calculations of the geometry structures, vibrational frequencies, and IR intensities strongly support the assignments. The CO activation mechanism has also been discussed. Our experimental and theoretical results schematically depict an activation process to CO dissociation.

Introduction

The study of carbon monoxide activation and dissociation is of considerable interest from an academic or an industrial viewpoint.[1] The interaction of carbon monoxide with transition metal atoms has been extensively studied.[2] Recent IR spectroscopic investigations of the reactions of laser-ablated early transition metal and actinide metal atoms with CO have demonstrated CO activation via transition metal and actinide metal carbonyl complexes.[3] The monocarbonyls of Nb, Th, and U can be isomerized to the inserted carbide oxide molecules on visible light irradiation. The dicarbonyls of the Ti group, the V group, and the actinide metals Th and U undergo photoinduced isomerization to the OMCCO (M = Ti, Zr, Hf, V, Nb, Ta, U, and Th) molecules with visible or UV photons. The OMCCO molecules can undergo further photochemical rearrangement to the $OTh(\eta^3\text{-CCO})$ or $(\eta^2\text{-}C_2)MO_2$ (M = Nb, Ta, and U) molecules with UV photons. Interestingly, the OCBBCO molecule undergoes successive photochemical rearrangements to form the OBBCCO isomer and finally the OBCCBO molecule, which offers a novel example of CO dissociation by the main-group elements.[4]

The long-standing goal of elucidating mechanisms of the catalyzed reactions has motivated numerous experimental investigations of CO chemisorption on transition metal surfaces.[1] Remarkably, the chemisorbed CO molecular state with unusual low C−O stretching frequencies (ν_{C-O}) (ca. 1200 cm^{-1}) has been found on some transition metal surfaces.[5] The so-called "bridging" and "semibridging" types of CO coordination have also been recognized and interpreted by several groups.[6] For instance, a low ν_{C-O} value (1330 cm^{-1}) was found for $(\eta^5\text{-}C_5H_5)_3Nb_3(CO)_7$.[6e] Even so, there has been no report so far on a simple homoleptic metal carbonyl molecule with a side-on-bonded CO and almost none is known with the structural configuration of CO as a precursor to dissociation. Recently, we communicated in a preliminary report $Sc_2[\eta^2(\mu_2\text{-C,O})]$ as the first dinuclear metal carbonyl with a side-on-bonded CO.[7] In this paper, we report a detailed matrix-isolation IR spectroscopic and density functional theory (DFT) study of the interactions of carbon monoxide molecules with the scandium and yttrium dimers, which show an activation process to CO dissociation.

Experimental and Theoretical Methods

The experiment for laser ablation and matrix isolation infrared spectroscopy is similar to those previously reported.[8] Briefly, the Nd:YAG laser fundamental (1064 nm, 10 Hz repetition rate with 10 ns pulse width) was focused on the rotating Sc and Y target. The laser-ablated metal atoms were co-deposited with CO in excess argon onto a CsI window cooled normally to 7 K by means of a closed-cycle helium refrigerator. Typically, 1−15 mJ/pulse laser power was used. $^{12}C^{16}O$ (99.95%), $^{13}C^{16}O$ (99%, ^{18}O < 1%), and $^{12}C^{18}O$ (99%) were used to prepare the CO/Ar mixtures. In general, matrix samples were deposited for 1−2 h with a typical rate of 2−4 mmol per hour. After sample deposition, IR spectra were recorded on a BIO-RAD FTS-6000e spectrometer at 0.5 cm^{-1} resolution using a liquid nitrogen cooled HgCdTe (MCT) detector for the spectral range of 5000−400 cm^{-1}. Samples were annealed at different temperatures and subjected to broad-band irradiation (λ > 250 nm) using a high-pressure mercury arc lamp (Ushio, 100 W).

Quantum chemical calculations were performed to predict the structures and vibrational frequencies of the observed reaction products using the Gaussian 03 program.[9] The BP86 and BPW91 density functional methods were used.[10] The 6-311++G(d,p) basis sets were used for C, O, and Sc atoms and SDD for Y atom.[11] Geometries were fully optimized, and

* To whom correspondence should be addressed. Electronic mail: q.xu@aist.go.jp.

10.1021/jp060269q CCC: $33.50
Published on Web 04/08/2006

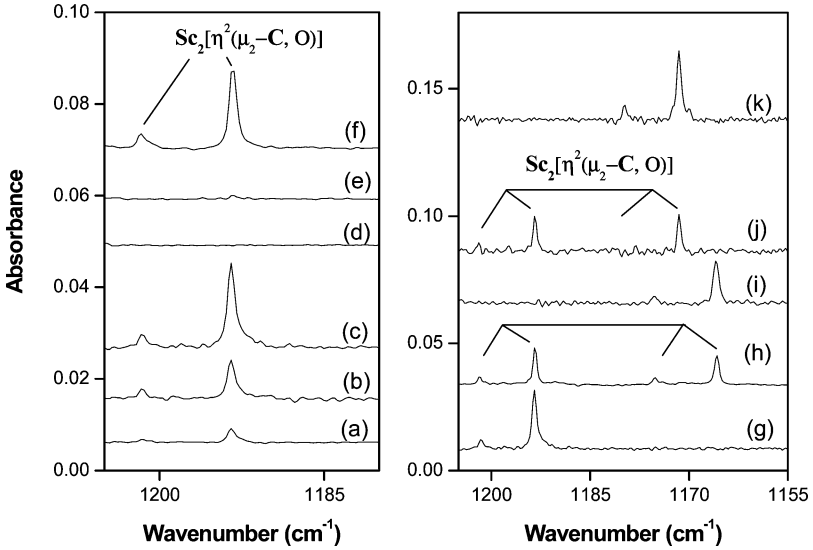

Figure 1. IR spectra in the 1210−1155-cm^{-1} region for laser-ablated Sc atoms co-deposited with CO in excess argon at 7 K. (a)−(f) with 0.06% CO: (a) 60 min of sample deposition, (b) after annealing to 28 K, (c) after annealing to 32 K, (d) after 20 min of broad-band irradiation, (e) after annealing to 36 K, (f) doping with 0.01% CCl_4, after annealing to 32 K; (g)−(k) with isotopic CO after annealing to 32 K: (g) 0.06% $^{12}C^{16}O$, (h) 0.03% $^{12}C^{16}O$ + 0.03% $^{13}C^{16}O$, (i) 0.06% $^{13}C^{16}O$, (j) 0.03% $^{12}C^{16}O$ + 0.03% $^{12}C^{18}O$, and (k) 0.06% $^{12}C^{18}O$.

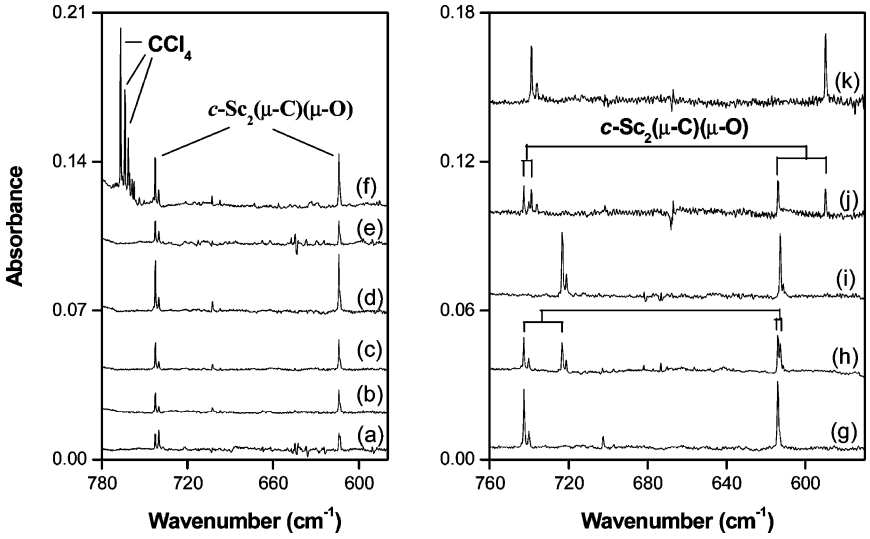

Figure 2. IR spectra in the 780−580-cm^{-1} region for laser-ablated Sc atoms co-deposited with CO in excess argon at 7 K. (a)−(f) with 0.06% CO: (a) 60 min of sample deposition, (b) after annealing to 28 K, (c) after annealing to 32 K, (d) after 20 min of broad-band irradiation, (e) after annealing to 36 K, (f) doping with 0.01% CCl_4, after 20 min of broad-band irradiation; (g)−(k) with isotopic CO after annealing to 32 K and broad-band irradiation for 20 min: (g) 0.06% $^{12}C^{16}O$, (h) 0.03% $^{12}C^{16}O$ + 0.03% $^{13}C^{16}O$, (i) 0.06% $^{13}C^{16}O$, (j) 0.03% $^{12}C^{16}O$ + 0.03% $^{12}C^{18}O$, and (k) 0.06% $^{12}C^{18}O$.

vibrational frequencies were calculated with analytical second derivatives. Transition-state optimizations were done with the QST3 algorithm within the synchronous transit-guided quasi-Newton (STQN) method, followed by the vibtrational calculations showing the obtained structures to be true saddle points. The intrinsic reaction coordinate (IRC) method was used to track minimum energy paths from transition structures to the corresponding local minima. A step size of 0.1 amu$^{1/2}$ bohr was used in the IRC procedure.

Results and Discussion

Experiments have been done with carbon monoxide concentrations ranging from 0.01 to 1.0% in excess argon. Typical IR spectra for the reactions of laser-ablated Sc and Y atoms with CO molecules in excess argon in the selected regions are illustrated in Figures1−3, and the absorption bands in different isotopic experiments are listed in Table 1. The stepwise annealing and photolysis behavior of the product absorptions is also shown in the figures and will be discussed below. Experiments were also done with doping CCl_4 of different concentrations serving as an electron scavenger in solid argon.

Quantum chemical calculations have been carried out for the possible isomers and electronic states of the potential product molecules. Note that the calculated results from BP86 and BPW91 methods are similar for scandium as previously reported,[7] whereas BPW91 is better for yttrium. Herein, mainly BPW91 results are presented for discussions. The optimized structures of the reaction products, intermediates, and transition states are shown in Figure 4. Figure 5 schematically presents the potential energy surface for the isomerization. Molecular orbital pictures of singlet $Sc_2[\eta^2(\mu_2\text{-C,O})]$, showing the lowest unoccupied molecular orbitals (LUMOs) and highest occupied molecular orbitals (HOMOs) down to the third valence molecular orbital from the HOMO, were plotted in Figure 6.

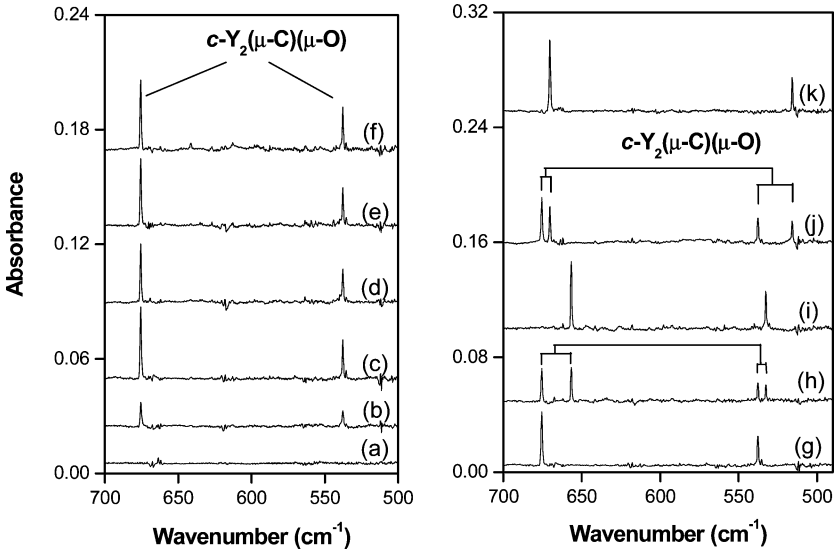

Figure 3. IR spectra in the 700−500 cm^{-1} region for laser-ablated Y atoms co-deposited with CO in excess argon at 7 K. (a)−(f) with 0.02% CO: (a) 60 min of sample deposition, (b) after annealing to 28 K, (c) after annealing to 32 K, (d) after 20 min of broad-band irradiation, (e) after annealing to 36 K, (f) doping with 0.01% CCl_4, after 20 min of broad-band irradiation; (g)−(k) with isotopic CO after annealing to 32 K and broad-band irradiation for 20 min: (g) 0.02% $^{12}C^{16}O$, (h) 0.01% $^{12}C^{16}O$ + 0.01% $^{13}C^{16}O$, (i) 0.02% $^{13}C^{16}O$, (j) 0.01% $^{12}C^{16}O$ + 0.01% $^{12}C^{18}O$, and (k) 0.02% $^{12}C^{18}O$.

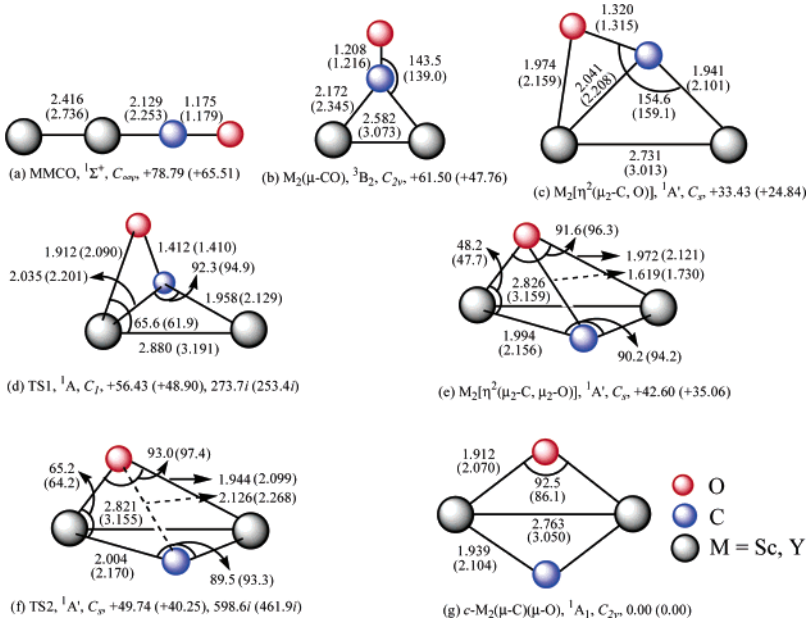

Figure 4. Optimized structures (bond lengths in angstroms, bond angles in degrees), electronic ground state, point group, and the relative energies (in kcal/mol) for the Sc_2CO and Y_2CO (in parentheses) isomers. For the transition states (TS, d and f), the letter "*i*" denotes the imaginary frequency (in cm^{-1}).

TABLE 1: IR Absorptions (in cm^{-1}) Observed from Co-deposition of Laser-Ablated Sc and Y Atoms with CO in Excess Argon at 7 K

$^{12}C^{16}O$	$^{13}C^{16}O$	$^{12}C^{18}O$	$^{12}C/^{13}C$	$^{16}O/^{18}O$	assignment	
1203.1	1175.2	1181.0	1.0237	1.0187	$Sc_2[\eta^2(\mu_2\text{-C,O})]$ site	C−O str.
1193.4	1165.8	1171.5	1.0237	1.0187	$Sc_2[\eta^2(\mu_2\text{-C,O})]$	C−O str.
742.6	723.3	738.9	1.0267	1.0050	c-$Sc_2(\mu\text{-C})(\mu\text{-O})$	Sc−C str.
740.3	721.2	736.6	1.0265	1.0050	c-$Sc_2(\mu\text{-C})(\mu\text{-O})$ site	Sc−C str.
614.1	612.9	589.8	1.0020	1.0412	c-$Sc_2(\mu\text{-C})(\mu\text{-O})$	Sc−O str.
675.6	656.8	670.4	1.0286	1.0078	c-$Y_2(\mu\text{-C})(\mu\text{-O})$	Y−C str.
537.8	532.8	515.9	1.0094	1.0425	c-$Y_2(\mu\text{-C})(\mu\text{-O})$	Y−O str.

$Sc_2[\eta^2(\mu_2\text{-C,O})]$. The IR spectra as a function of changes of CO concentrations and laser energies are of particular interest here. With high CO concentration (0.50%) and low laser energy (3 mJ/pulse), $ScCO^+$ (1924.1 cm^{-1}) and $Sc(CO)_n$ (n = 1−4) (1834.9; 1852.8, 1778.2, 1717.0; 1822.7; and 1865.6 cm^{-1}) are the primary products upon sample deposition (not shown here), which have been previously identified.[12] New absorptions were produced on sample deposition with lower CO concentration (0.06%) and higher laser power (12 mJ/pulse) (Table 1 and Figures 1 and 2). The 1203.1- and 1193.4-cm^{-1} bands increased on sample annealing, disappeared after broad-band irradiation, and did not recover upon further annealing. On the basis of the

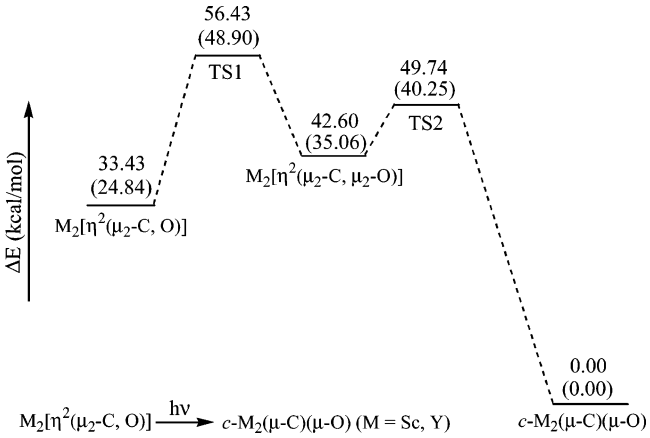

Figure 5. Potential energy surface (PES) of the $M_2[\eta^2(\mu_2\text{-C,O})] \rightarrow c\text{-}M_2(\mu\text{-C})(\mu\text{-O})$ reactions for the scandium and yttrium (in parentheses) dimers.

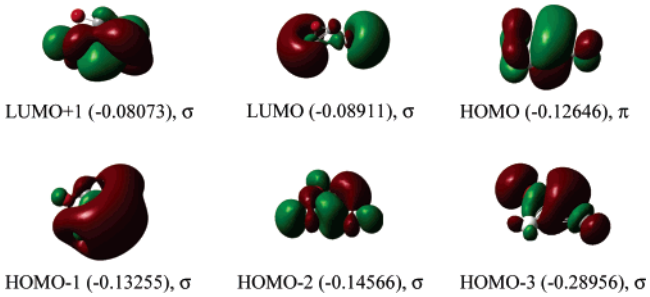

Figure 6. Molecular orbital pictures of singlet $Sc_2[\eta^2(\mu_2\text{-C,O})]$, showing the LUMO+1, LUMO, and HOMO down to the third valence molecular orbital from the HOMO. The unit of orbital energy is hartree (in parentheses).

growth/decay characteristics as a function of changes of experimental conditions, the absorptions in the 1180−1210-cm^{-1} region can be grouped together to one species. Note that the new bands were only observed with lower CO concentration and higher laser power than those for mononuclear Sc carbonyls, indicating that the new products involve more than one Sc atom. Doping with CCl_4 as an electron scavenger has no effect on these bands, indicating that the products are neutral (Figure 1).

The 1203.1- and 1193.4-cm^{-1} absorptions shifted to 1175.2 and 1165.8 cm^{-1} with $^{13}C^{16}O$ and to 1181.0 and 1171.5 cm^{-1} with $^{12}C\,^{18}O$, respectively (Table 1 and Figure 1), exhibiting isotopic frequency ratios ($^{12}C^{16}O/^{13}C^{16}O$: 1.0237 and 1.0237; $^{12}C\,^{16}O/^{12}C\,^{18}O$: 1.0187 and 1.0187) characteristic of C−O stretching vibrations. In the mixed $^{12}C^{16}O + {}^{13}C^{16}O$ and $^{12}C\,^{16}O + {}^{12}C\,^{18}O$ experiments (Figure 1), only pure isotopic counterparts were observed, indicating that only one CO subunit is involved. Therefore, the absorptions at 1203.1 and 1193.4 cm^{-1} are due to the C−O stretching of a species having a Sc_x-CO stoichiometry with $x \geq 2$ in different matrix sites.

DFT calculations have been performed for Sc_xCO ($x = 1-4$) for all the possible isomers. The reliability trial calculations show that the ν_{C-O} value for the linear ScCO are 1843.3 (BP86) and 1852.6 (BPW91) cm^{-1}, respectively, in excellent agreement with the present experiments and previous reports.[7] The calculations show that only $Sc_2[\eta^2(\mu_2\text{-C,O})]$ (Figure 4), a unique molecule with a single bridging CO that is tilted to the side, nicely matches the experimental vibrational frequencies, relative absorption intensities, and isotopic shifts in the 1180−1210 cm^{-1} region. At the BPW91/6-311++G(d,p) level, the ν_{C-O} value of $Sc_2[\eta^2(\mu_2\text{-C,O})]$ is 1240.4 cm^{-1} (Table 2), whereas that of $Sc_3[\eta^2(\mu_3\text{-C}, \mu_2\text{-O})]$ is predicted to be 1032.4 cm^{-1} and that of $Sc_4[\eta^2(\mu_3\text{-C}, \mu_3\text{-O})]$ to be 1070.9 cm^{-1}, respectively.

The excellent agreement between experimental and calculated vibrational frequencies, relative absorption intensities, and isotopic shifts points to the identification of the 1193.4 cm^{-1} absorption as the C−O stretching of $Sc_2[\eta^2(\mu_2\text{-C,O})]$. The calculated $^{12}C^{16}O/^{13}C^{16}O$ and $^{12}C^{16}O/^{12}C^{18}O$ frequency ratios of $Sc_2[\eta^2(\mu_2\text{-C,O})]$ are 1.0252 and 1.0197, in accord with the observed values (1.0237 and 1.0187) (Table 2). The Sc−Sc stretching is predicted to be 219.5 cm^{-1}, which is beyond the present spectral range of 5000−400 cm^{-1}. The Sc−C and Sc−O stretching frequencies of $Sc_2[\eta^2(\mu_2\text{-C,O})]$ are predicted to be 663.0 and 546.7 cm^{-1}, respectively, while their intensities (1 and 15 km/mol) are too small to be detected.

BPW91 calculations predict that $Sc_2[\eta^2(\mu_2\text{-C,O})]$ has a $^1A'$ ground state and C_s symmetry with a Sc−O bond of 1.974 Å and two unequivalent Sc−C bonds of 1.941 and 2.041 Å in the same plane (Figure 4). The calculated $^{12}C^{16}O/^{13}C^{16}O$ and $^{12}C\,^{16}O/^{12}C^{18}O$ frequency ratios of $Sc_2[\eta^2(\mu_2\text{-C,O})]$ are 1.0251 and 1.0198, in good agreement with the observed values (1.0237 and 1.0187) (Table 2). CO leans toward the two Sc atoms with ∠Sc−C−O of 154.6°. In contrast, the $\eta^2(\mu_3\text{-C},\mu_2\text{-O})$ ligand in $(\eta^5\text{-}C_5H_5)_3Nb_3(CO)_7$ leans toward the Nb(1)−Nb(2) vector, with ∠Nb(3)−C−O of 169.6° and R_{C-O} of 1.303 Å.[6e] An analogous Mn−C−N unit with ∠Mn−C−N of 168° is observed in $(\mu\text{-}p\text{-}CH_3C_6H_4NC)Mn_2(Ph_2PCH_2PPh_2)_2(CO)_4$.[6f] The R_{C-O} in $Sc_2[\eta^2(\mu_2\text{-C,O})]$ (1.320 Å) is longer than that in $OSc(\eta^2\text{-CO})$ (1.211 Å).[13]

In the present experiments on the reaction of laser-ablated Y atoms with CO molecules, however, no absorptions for the analogous $Y_2[\eta^2(\mu_2\text{-C,O})]$ product were observed.

***c*-$M_2(\mu\text{-C})(\mu\text{-O})$ (M = Sc, Y).** In the Sc + CO experiments (Figure 2), new bands at 742.6, 740.3, and 614.1 cm^{-1} slightly increased on annealing, markedly increased upon broad-band irradiation at the expense of the 1203.1 and 1193.4 cm^{-1} absorptions of $Sc_2[\eta^2(\mu_2\text{-C,O})]$, and observably decreased on further annealing. The 742.6- and 740.3-cm^{-1} bands showed very small shifts with $^{12}C^{18}O$ (3.7 and 3.7 cm^{-1}) but shifted to 723.3 and 721.2 cm^{-1} with $^{13}C^{16}O$. The $^{12}C^{16}O/^{13}C^{16}O$ frequency ratios of 1.0267 and 1.0265 (Table 1) imply that these bands are mainly due to a Sc−C stretching of the same species in different matrix sites. The 614.1-cm^{-1} band showed a very small shift with $^{13}C^{16}O$ (1.2 cm^{-1}) but a large shift with $^{12}C^{18}O$ (24.3 cm^{-1}). The $^{12}C^{16}O/^{12}C^{18}O$ frequency ratio of 1.0412 indicates that the 614.1-cm^{-1} band is mainly due to a Sc−O stretching. The mixed isotopic spectra (Figure 2) showed that only one C and one O atom, which are separated from each other, are

TABLE 2: Comparison of Observed and Calculated IR Frequencies (cm^{-1}) for the Products

		observed			calculated		
species	mode	freq	$^{12}C/^{13}C$	$^{16}O/^{18}O$	freq	$^{12}C/^{13}C$	$^{16}O/^{18}O$
$Sc_2[\eta^2(\mu_2\text{-C,O})]$	ν_{C-O}	1193.4	1.0237	1.0187	1240.4	1.0251	1.0198
$c\text{-}Sc_2(\mu\text{-C})(\mu\text{-O})$	ν_{Sc-C}	742.6	1.0267	1.0050	756.9	1.0264	1.0065
$c\text{-}Sc_2(\mu\text{-C})(\mu\text{-O})$	ν_{Sc-O}	614.1	1.0020	1.0412	603.3	1.0067	1.0375
$c\text{-}Y_2(\mu\text{-C})(\mu\text{-O})$	ν_{Y-C}	675.6	1.0286	1.0078	674.2	1.0290	1.0078
$c\text{-}Y_2(\mu\text{-C})(\mu\text{-O})$	ν_{Y-O}	537.8	1.0094	1.0425	524.4	1.0147	1.0364

involved. The 742.6- and 614.1-cm^{-1} absorptions are assigned to the Sc−C and Sc−O stretching vibrations of *c*-$Sc_2(\mu$-C)(μ-O), respectively.[7]

In the Y + CO experiments (Figure 3), similar absorptions at 675.6 and 537.8 cm^{-1} have been observed, which are assigned to the Y−C and Y−O stretching vibrations of *c*-$Y_2(\mu$-C)(μ-O). The 675.6-cm^{-1} band shifted to 656.8 cm^{-1} with $^{12}C^{18}O$ and to 670.4 cm^{-1} with $^{13}C^{16}O$, giving the $^{12}C^{16}O/^{13}C^{16}O$ and $^{12}C^{16}O/^{12}C^{18}O$ frequency ratios of 1.0286 and 1.0078, respectively. The 537.8-cm^{-1} band showed a very small shift with $^{13}C^{16}O$ (1.2 cm^{-1}) but a large shift with $^{12}C^{18}O$ (21.9 cm^{-1}). The doublet isotopic structures have been observed in the mixed isotopic spectra (Figure 3).

As shown in Figure 4, our DFT calculations predict that the *c*-$M_2(\mu$-C)(μ-O) (M = Sc, Y) molecules have a $^1A_1$ ground state with C_{2v} symmetry. Taking *c*-$Sc_2(\mu$-C)(μ-O) as an example, the Sc−C and Sc−O bond lengths are predicted to be 1.939 and 1.912 Å, respectively. The calculated ν_{Sc-C} is 756.9 cm^{-1} and the calculated $^{12}C^{16}O/^{13}C^{16}O$ and $^{12}C^{16}O/^{12}C^{18}O$ frequency ratios are 1.0264 and 1.0065, consistent with the observed ν_{Sc-C} (742.6 cm^{-1}) and frequency ratios (1.0267 and 1.0050) (Table 2). Similar theoretical supports for the identification of *c*-$Sc_2(\mu$-C)(μ-O) hold true for the Sc−O stretching vibration (Table 2). In contrast to the observable Sc−C vibration (756.9 cm^{-1}, 70 km/mol) and Sc−O vibration (603.3 cm^{-1}, 121 km/mol), other vibrational modes in *c*-$Sc_2(\mu$-C)(μ-O) are predicted to be 693.4 (5 km/mol), 451.7 (2 km/mol), 398.8 (0.2 km/mol), and 233.6 (82 km/mol) cm^{-1}, in which the first two modes are too small to be detected and the last two modes are beyond the present spectral range of 5000−400 cm^{-1}. Similar calculated results has also been obtained for *c*-$Y_2(\mu$-C)(μ-O) as summarized in Table 2.

Reaction Mechanism. The BPW91 calculated results show that $Sc_2[\eta^2(\mu_2$-C,O)] lies 33.43 kcal/mol above its most stable C−O-dissociated isomer, *c*-$Sc_2(\mu$-C)(μ-O), whereas the terminal-bonded ScScCO and bridge-bonded $Sc_2(\mu$-CO) isomers are 78.79 and 61.50 kcal/mol higher than *c*-$Sc_2(\mu$-C)(μ-O), respectively (Figure 4). From the $Sc_2[\eta^2(\mu_2$-C,O)] molecule, the reaction proceeds by binding oxygen atom with another scandium atom to form a nonplanar intermediate $Sc_2[\eta^2(\mu_2$-C,μ_2-O)] via transition state TS1. It is predicted that $Sc_2[\eta^2(\mu_2$-C,μ_2-O)] lies 42.60 kcal/mol higher in energy than *c*-$Sc_2(\mu$-C)(μ-O). From $Sc_2[\eta^2(\mu_2$-C,O)] to $Sc_2[\eta^2(\mu_2$-C,μ_2-O)], the C−O bond elongates by 0.299 Å. The barrier height for this process is predicted to be 23.00 kcal/mol (Figure 5), which can be obtained by ultraviolet visible irradiation. The vibrational mode of the imaginary frequency of TS1 (273.7*i* cm^{-1}) corresponds to the transition motion leading to the Sc−O formation. The transition state optimization was followed by the frequency and IRC calculations at the BPW91/6-311++G(d,p) level of theory, which confirmed that TS1 does connect $Sc_2[\eta^2(\mu_2$-C,O)] and the nonplanar $Sc_2[\eta^2(\mu_2$-C,μ_2-O)] intermediate. From $Sc_2[\eta^2(\mu_2$-C,μ_2-O)], CO can further be activated to form the C−O-dissociated *c*-$Sc_2(\mu$-C)(μ-O) product via transition state TS2. The C−O distance in the TS2 is 2.126 Å. The vibrational mode of the imaginary frequency of TS2 (598.6*i* cm^{-1}) corresponds to the transition motion leading to the cleavage of the C−O bond. The calculated BPW91/6-311++G(d,p) energies place transition state TS2 7.14 kcal/mol higher in energy than $Sc_2[\eta^2(\mu_2$-C, μ_2-O)] (Figure 5). The BPW91/6-311++G(d,p) IRC calculation confirmed TS2 does connect the nonplanar $Sc_2[\eta^2(\mu_2$-C,μ_2-O)] intermediate and the *c*-$Sc_2(\mu$-C)(μ-O) product.

As illustrated in Figure 6, the HOMO of $Sc_2[\eta^2(\mu_2$-C,O)] is π-type bond, which comprises the Sc_2 $3\pi_u \rightarrow$ CO 2π back-bonding, leading to the weakening of the C−O bond. The HOMO-1 is largely Sc_2 $6\sigma_u$ in character and is nonbonding, and HOMO-2 and HOMO-3 are σ-type bonds. Similar results have also been obtained for yttrium.

In addition to scandium, the process starting with the interaction of CO with metal and ending with CO dissociation by the lanthanum dimer has also fortunately been captured by the laser-ablation matrix-isolation technique,[14] while no $Y_2[\eta^2(\mu_2$-C,O)] molecule has been observed for yttrium. By consideration that laser ablation of the metal target produces the plume of radiation and the samples are deposited with concurrent irradiation,[2,15] the *c*-$Y_2(\mu$-C)(μ-O) molecule may be formed from the reaction of CO with "energetic" Y atoms produced by laser ablation. The potential $Y_2[\eta^2(\mu_2$-C,O)] molecule might be hopefully generated using thermal evaporation technique.

Anomalous C−O bond weakening has been reported for chemisorbed CO in side-on-bonded modes on transition metal surfaces as model catalysts, for which the ν_{C-O} values were observed around 1100−1400 cm^{-1}.[5] Interestingly, the structures of Sc_2CO isomers in Figure 4 represent almost all the main modes of metal−CO coordination to date. The present observation schematically depicts the whole process starting with the interaction of CO with metal to CO dissociation. The present finding is a key for explaining the unusually low ν_{C-O} values (1100−1400 cm^{-1}) of the chemisorbed CO molecules on transition metal surfaces[5] and for understanding the activation process to CO dissociation on metal catalysts.

Conclusion

Reactions of laser-ablated scandium and yttrium atoms with dilute carbon monoxide molecules in solid argon have been investigated using matrix-isolation IR spectroscopy. In the Sc + CO experiments, the absorption at 1193.4 cm^{-1} is assigned to the C−O stretching vibration of the $Sc_2[\eta^2(\mu_2$-C,O)] molecule on the basis of the results of the isotopic substitution, the change of laser power and CO concentration, and the comparison with DFT calculations. This CO-activated molecule undergoes ultraviolet−visible photoinduced rearrangement to the CO-dissociated molecule, *c*-$Sc_2(\mu$-C)(μ-O). The infrared absorptions of the products are accurately predicted by quantum chemical calculations. Our experimental and theoretical results schematically depict an activation process to CO dissociation. Similar argon matrix experiments with yttrium give the CO-dissociated *c*-$Y_2(\mu$-C)(μ-O) molecule. The potential $Y_2[\eta^2(\mu_2$-C,O)] molecule might be hopefully generated using thermal evaporation technique.

Acknowledgment. The authors would like to express thanks to the reviewers for valuable suggestions. This work was supported by a Grant-in-Aid for Scientific Research (B) (Grant No. 17350012) from the Ministry of Education, Culture, Sports, Science and Technology (MEXT) of Japan and by the Marubun Research Promotion Foundation. L.J. thanks the MEXT of Japan and Kobe University for an Honors Scholarship.

References and Notes

(1) Cotton, F. A.; Wilkinson, G.; Murillo, C. A.; Bochmann, M. *Advanced Inorganic Chemistry*, 6th ed.; Wiley: New York, 1999. Rhodin, T. N.; Ertl, G. *The Nature of the Surface Chemical Bond*; North-Holland: Amsterdam, 1979. King, D. A.; Woodruff, D. P. *The Chemical Physics of Solid Surfaces and Heterogeneous Catalysis*; Elsevier Press: Amsterdam, 1991.

(2) Zhou, M. F.; Andrews, L.; Bauschlicher, C. W., Jr. *Chem. Rev.* **2001**, *101*, 1931 and references therein.

(3) Zhou, M. F.; Andrews, L.; Li, J.; Bursten, B. E. *J. Am. Chem. Soc.* **1999**, *121*, 12188. Li, J.; Bursten, B. E.; Zhou, M. F.; Andrews, L. *Inorg. Chem.* **2000**, *40*, 5448. Zhou, M. F.; Andrews, L.; Li, J.; Bursten, B. E. *J. Am. Chem. Soc.* **1999**, *121*, 9712. Zhou, M. F.; Andrews, L. *J. Phys. Chem. A* **1999**, *103*, 7785. Zhou, M. F.; Andrews, L. *J. Am. Chem. Soc.* **2000**, *122*, 1531.

(4) Zhou, M. F.; Jiang, L.; Xu, Q. *Chem.−Eur. J.* **2004**, *10*, 5817.

(5) Moon, D. W.; Bernasek, S. L.; Dwyer, D. J.; Gland, J. L. *J. Am. Chem. Soc.* **1985**, *107*, 4363. Sinn, N. D.; Madey, T. E. *Phys. Rev. Lett.* **1984**, *53*, 2481. Hoffmann, F. M.; de Paola, R. A. *Phys. Rev. Lett.* **1984**, *52*, 1697.

(6) (a) Cotton, F. A. *Prog. Inorg. Chem.* **1976**, *21*, 1 and references therein. (b) Cotton, F. A.; Frenz, B. A.; Kruczynski, L. *J. Am. Chem. Soc.* **1973**, *95*, 951. *J. Organomet. Chem.* **1978**, *160*, 93. (c) Manassero, M.; Sansoni, M.; Longoni, G. *J. Chem. Soc., Chem. Commun.* **1976**, 919. (d) Colton, R.; McCormick, M. J. *Coord. Chem. Rev.* **1980**, *31*, 1. (e) Herrmann, W. A.; Biersack, H.; Ziegler, M. L.; Weidenhammer, K.; Siegel, R.; Rehder, D. *J. Am. Chem. Soc.* **1981**, *103*, 1692. (f) Benner, L. S.; Olmstead, M. M.; Balch, A. L. *J. Organomet. Chem.* **1978**, *159*, 289.

(7) A preliminary report of the $Sc_2[\eta^2(\mu_2\text{-}C,O)]$ and *c*-$Sc_2(\mu\text{-}C)(\mu\text{-}O)$ molecules has been communicated, see: Jiang, L.; Xu, Q. *J. Am. Chem. Soc.* **2005**, *127*, 42.

(8) Burkholder, T. R.; Andrews, L. *J. Chem. Phys.* **1991**, *95*, 8697. Zhou, M. F.; Tsumori, N.; Andrews, L.; Xu, Q. *J. Phys. Chem. A* **2003**, *107*, 2458. Jiang, L.; Xu, Q. *J. Chem. Phys.* **2005**, *122*, 034505.

(9) Frisch, M. J.; Trucks, G. W.; Schlegel, H. B.; Scuseria, G. E.; Robb, M. A.; Cheeseman, J. R.; Montgomery, J. A., Jr.; Vreven, T.; Kudin, K. N.; Burant, J. C.; Millam, J. M.; Iyengar, S. S.; Tomasi, J.; Barone, V.; Mennucci, B.; Cossi, M.; Scalmani, G.; Rega, N.; Petersson, G. A.; Nakatsuji, H.; Hada, M.; Ehara, M.; Toyota, K.; Fukuda, R.; Hasegawa, J.; Ishida, M.; Nakajima, T.; Honda, Y.; Kitao, O.; Nakai, H.; Klene, M.; Li, X.; Knox, J. E.; Hratchian, H. P.; Cross, J. B.; Adamo, C.; Jaramillo, J.; Gomperts, R.; Stratmann, R. E.; Yazyev, O.; Austin, A. J.; Cammi, R.; Pomelli, C.; Ochterski, J. W.; Ayala, P. Y.; Morokuma, K.; Voth, G. A.; Salvador, P.; Dannenberg, J. J.; Zakrzewski, V. G.; Dapprich, S.; Daniels, A. D.; Strain, M. C.; Farkas, O.; Malick, D. K.; Rabuck, A. D.; Raghavachari, K.; Foresman, J. B.; Ortiz, J. V.; Cui, Q.; Baboul, A. G.; Clifford, S.; Cioslowski, J.; Stefanov, B. B.; Liu, G.; Liashenko, A.; Piskorz, P.; Komaromi, I.; Martin, R. L.; Fox, D. J.; Keith, T.; Al-Laham, M. A.; Peng, C. Y.; Nanayakkara, A.; Challacombe, M.; Gill, P. M. W.; Johnson, B.; Chen, W.; Wong, M. W.; Gonzalez, C.; Pople, J. A. *Gaussian 03*, revision B.04; Gaussian, Inc.: Pittsburgh, PA, 2003.

(10) Becke, A. D. *Phys. Rev. A* **1988**, *38*, 3098. Perdew, J. P. *Phys. Rev. B* **1986**, *33*, 8822. Perdew, J. P.; Burke, K.; Wang, Y. *Phys. Rev. B* **1996**, *54*, 16533.

(11) McLean, A. D.; Chandler, G. S. *J. Chem. Phys.* **1980**, *72*, 5639. Krishnan, R.; Binkley, J. S.; Seeger, R.; Pople, J. A. *J. Chem. Phys.* **1980**, *72*, 650. Frisch, M. J.; Pople, J. A.; Binkley, J. S. *J. Chem. Phys.* **1984**, *80*, 3265. Wachters, A. J. H. *J. Chem. Phys.* **1970**, *52*, 1033. Hay, P. J. *J. Chem. Phys.* **1977**, *66*, 4377. Dunning, T. H., Jr.; Hay, P. J. *Modern Theoretical Chemistry*; Schaefer, H. F., III, Ed.; Plenum: New York, 1976; Vol. 3, p 1.

(12) Zhou, M. F.; Andrews, L. *J. Phys. Chem. A* **1999**, *103*, 2964.

(13) Zhou, M. F.; Andrews, L. *J. Am. Chem. Soc.* **1998**, *120*, 13230.

(14) Xu, Q.; Jiang, L.; Zou, R. Q. *Chem.−Eur. J.* in press.

(15) Himmel, H. J.; Downs, A. J.; Greene, T. M. *Chem. Rev.* **2002**, *102*, 4191 and references therein. Jiang, L.; Xu, Q. *J. Am. Chem. Soc.* **2005**, *127*, 8906.